

Dehydration-dehydrogenation Activities of 2-Propanol over Fe₂O₃ / TiO₂ Catalysts: Effect of Li⁺ Impregnation

E. A. El-Sharkawy and Shar S. Al-Shihry

*Department of Chemistry, College of Science
P.O. Box 1759, King Faisal University
Hofuf 31982, Eastern Province, Saudi Arabia*

(Received 18-2-1423H.; accepted for publication on 22-12-1423H.)

Abstract. Fe₂O₃/TiO₂ binary solid catalysts containing 1-35 wt.% Fe were prepared by impregnating TiO₂ with Fe (NO₃)₃ at 333K, followed by, drying and calcination at 873K. Li impregnated Fe₂O₃ / TiO₂ samples containing 1-10 wt.% Li was also prepared followed the same procedure. The textural properties were determined from the low temperature adsorption of nitrogen at 77K. The structural characteristics of pre-calcined samples were examined by using various techniques, including, X-ray diffraction (XRD), differential thermal analysis (DTA), thermal gravimetric analysis (TGA) and ESR techniques. The determination of surface acidity was performed by the adsorption of n-butyl amine in non-aqueous media. The catalytic conversion of 2-propanol as well as the reaction kinetics was performed using the microcatalytic pulse technique. The measurable textural parameters including surface area and the total pore volume decreased continuously by increasing % loading of Fe or Li. XRD technique revealed that TiO₂, Fe₂O₃, TiFe₂O₄ and Li₂Fe₂O₄ typical spinels were assigned. ESR shows the presence of ferric iron (III) belonging to iron oxide and iron spinel. Regarding with surface acidity, it was found that the values of acid amount increased with the increases of % Fe loading, while the addition of Li exhibits an opposite behavior. The catalytic activity was influenced to more or less extent by the %loading of iron and/or Li-oxides and also by surface acidity of the investigated catalysts.

Introduction

Mixed oxides including binary and ternary system have long attracted attention since they possess unique catalytic properties in comparison to those of individual metal oxide [1,2]. Such behavior may be arisen from the interaction between the supported oxide and the support may lead to a structural and chemical changes [3,4]. Titania and Metal oxides supported TiO₂ are catalytically active for a great variety of reactions, including

* Permanent address: Chemistry Department, College of Education at Al-Arish, Suez Canal University, Egypt.

among the other, oligomerizations [5], selective catalytic reduction of nitrogen containing compounds [6,7], hydrogenation reaction [8], etc. Iron-titania has a significant interest because of its use as a photoactive catalyst (9-11). Studying of the textural characteristics as well as the complete knowledge about the structural characteristic of the catalyst has been recognized as important features in understanding the catalytic behavior.

However, the correlation between the chemical composition, catalyst structure, acidic properties and catalytic activity is also very important for the development of scientific criteria in catalyst application. A considerable amount of research has been devoted to correlate the catalytic activity and surface acidity for Fe – Titania catalysts (4, 12, 13). In fact no conclusions were certificated for the reported literatures in this concern.

The present work attempted to: (i) determine the textural properties of Fe_2O_3 - TiO_2 as well as Li impregnated system from the low temperature adsorption of N_2 at 77 K, (ii) investigate the structural characteristics of the prepared catalysts, (iii) examine the acidic properties of the calcined samples, and (iv) correlate the acidic and/or textural properties of these systems to the catalytic conversion of 2-propanol.

Experimental

Preparation of catalysts

Fe_2O_3 supported on TiO_2 was prepared by impregnating TiO_2 (Strem Chemicals, 99.9% purity) with aqueous solution of iron nitrate, containing the appropriate amount of Fe_2O_3 (1,5,10,20 and 35 wt. % Fe_2O_3), with continuous vigorous stirring at 333.0 K. The water was removed by evaporation with permanent stirring, while the resulting solid was dried overnight at 393 K and then calcined at 923 K for 24 hrs.

Lithium impregnated $\text{Fe}_2\text{O}_3/\text{TiO}_2$ samples were also prepared by co-impregnating TiO_2 with aqueous solution containing lithium nitrate and iron nitrate. The aqueous solutions were adjusted to contain only the same concentration of iron nitrate (20 wt. % Fe_2O_3) and different concentration of lithium nitrate, giving 1,3,6,10 wt. % Li_2O . Li impregnated samples received the same treatments described latter for the preparation of Fe_2O_3 - TiO_2 . The resulting samples have been designated according to their content of Fe and Li. The letter T, F and L were indicated for titania, iron oxide and lithium oxide, respectively. The Roman numbers I, II, III, IV and V are designated to 1,5,10,20 and 35wt% Fe_2O_3 , whereas the Arabic number 1,3,6 and 10 indicates Li contents. Thus, the sample TFI refers to Fe_2O_3 - TiO_2 sample containing 1.0 wt. % Fe_2O_3 , whereas TFIVL10 refers to the catalyst containing 20 wt. % Fe_2O_3 and 10 wt.% Li_2O .

Techniques

Nitrogen physisorption: Nitrogen physisorption, using sorbimetric glass system, at lower temperature of 77 K was used to evaluate the textural parameters for the calcined

catalysts, e.g. surface area and total pore volume. Prior to the adsorption measurement, the sample was in situ activated at 573 K and a reduced pressure of 10^{-6}

X-ray diffraction (XRD): X-ray diffraction (XRD) patterns of the precalcined samples were recorded with the aid of a Siemens Rigaku "Geiger flux" D/max 1A apparatus, employing Ni-filtered Cu radiation ($\lambda = 1.5405 \text{ \AA}$). The diffraction was scanned within the intervals $2\theta = 12-80$ at scan rate of $2^\circ / \text{min}$.

Thermal gravimetric analysis (TGA): TGA of TFIV, TFIVL10, TFV samples were studied using the thermolyser of Shimadzu TGA-50 H type, at a heating rate of 273 K min^{-1} and $\alpha\text{-Al}_2\text{O}_3$ was used as an inert reference.

Electron spin resonance (ESR): The ESR spectra were recorded on Bruker EMX spectrometer at 298 K, operating in the X-band. The operating parameters including the sweep width of 3000 G, Resolution 1024 points, Frequency 9.756 GHz, moderation frequency 100 KHz, moderation amplitude 5.0 G and power of 0.201 mW were adjusted.

Surface acidity measurements: The surface acidity of the examined solids was determined spectrophotometrically according to the reported method (14). The sample was preheated for 4 hrs at 393 K prior to the adsorption measurements. The adsorption measurements was performed in non-aqueous media by shaking 25 ml of n-butylamine/cyclohexane solution containing 0.1 g sample for 2 hrs to attain the equilibrium condition. The concentration of unadsorbed n-butylamine was determined spectrophotometrically, and therefore the amount of the adsorbed organic base could be mathematically evaluated.

Catalytic activity measurements: The catalytic tests were carried out using the micro catalytic pulse technique, where a fixed-bed micro catalytic reactor of 10 mm i.d. containing 0.2 g. catalyst. The catalyst was in situ electrically activated at 773 K for 3 hrs in a flow of nitrogen of 23 ml/min. The reactor is attached online to the analytical column of 104 PyUnicam gas chromatography. 3 μl dose of 2-propanol was injected on to the catalyst in the N_2 stream, while the gaseous products were analyzed by gas chromatography. The kinetics of catalytic conversion of 2-propanol was investigated within N_2 flow of 16.6-47 ml/min.

Results and Discussion

Textural characterization: The adsorption/desorption isotherms of N_2 at 77 K on the investigated samples were specified by the type II, according to BDDT classification. The desorption branches were of type H_3 hysteresis of slight shaped pores. The meniscus is not formed until a high P/P° is obtained, where the desorption took place by evaporation from cylindrical meniscus. The mathematical treatment of the adsorption data, using BET equation (15) and adopting 0.162 nm^2 as cross-sectional area of N_2 molecule, the values of specific surface area S_{BET} (m^2/g), V_{T} (ml/g) and the mean pore radius (r) can be calculated, Table 1.

Table 1. Textural characteristics of the investigated catalysts

Catalyst	S_{BET} (m ² /g)	V_{T} (ml/g)	r' (nm) for 4 hrs.
T	17.1	0.15	17.5
TFI	19.1	0.17	17.8
TFII	15.2	0.12	15.8
TFIII	13.4	0.09	13.4
TFIV	18.9	0.17	18.0
TFV	16.0	0.130	16.3
TFIVL1	17.0	0.135	15.9
TFIVL3	12.8	0.074	11.6
TFIVL6	9.10	0.049	10.8
TFIVL10	7.00	0.023	6.60

$$V_{\text{T}} \text{ (ml/g)} = V_{\text{saturation}} \times 15.47 \times 10^{-4} \text{ and } r' \text{ (nm)} = (2 V_{\text{T}} / S_{\text{BET}}) \times 10^3$$

Concerning with the depicted the data in Table 1, it reveals that:

1. The thermal decomposition of iron nitrate, (1.0 wt.% Fe₂O₃), impregnated with TiO₂, led to a creating of new pores, thus increasing the values of V_{T} and therefore S_{BET} .
2. The successive increasing of iron content up to 20 wt. % Fe₂O₃ was associated with a gradual decrease of S_{BET} , as well as V_{T} . This may be arisen from the partial blocking of the pores (4, 16).
3. The increase of surface area for 20 wt. % Fe₂O₃ may be attributed to the attack of Fe₂O₃ to the walls of some wider pores, enhancing the formation of some micropores (17),
4. The effect of Li⁺ impregnation on the evaluated S_{BET} of Fe₂O₃/TiO₂ system act on the same way as the impregnation of Fe³⁺. This may be speculated from the great probability of thermal diffusion of small sized ions, e.g. Li in our investigation, into the lattice structure to block some of the created pore and leading thus to a decrease of surface area.

Structural characterization

X-ray diffraction (XRD): Matching of the recorded XRD lines with the d-plane spacing identified the crystalline structure of the investigated samples. The XRD patterns of the 923 K pre-calcined T, TFIV and TFV are shown. The inspection of these patterns indicated the assignment of crystalline rutile TiO₂ structure with the characteristics 2θ at 24, 36.4, 37, 37.9, 47.2, 53.2, 54.2, 61.6, 62, 68.1, 69.68, 74.4 and 75.2. The increase of Fe₂O₃ content was accompanied with a decrease of TiO₂ crystallinity, whereas the crystallinity of α -Fe₂O₃ increased. TiO₂ supported Fe₂O₃ exhibited a weak XRD characteristic lines at 2θ of 34, 34.8, 35.2, 40.6, 46.8, 57.4, 58.5 and 71.8, attributing to the formation of α -Fe₂O₃ (15). In addition to the latter phases, TiFe₂O₅ was also detected at 2θ of 32.8 and 49 (18).

Thermal treatment of Li-impregnated iron-titania led to an appreciable interaction between Li₂O and Fe₂O₃, thus forming Li₂Fe₂O₄. XRD patterns describe this

interaction, where the recorded XRD lines located at $2\theta = 30, 37.4, 43.2$ and 57.0 may be referred to the formation of LiFeO_2 . The formation of the latter phase as the monomeric structure may be developed via the thermal decomposition of $\text{Li}_2\text{Fe}_2\text{O}_4$, particularly at elevated calcinations temperature. It remains now to point out that, the degree of crystallinity of LiFeO_2 phase was gradually enhanced upon increasing the content of Li impregnant.

Electron spin resonance (ESR): The ESR spectrum of TF shows a superposition of two signals representing different structural environments for the Fe^{3+} ion. It has been reported that, ferric iron can give rise to a wide intervals of effective g values, depending on the fine structural parameters of the catalyst (19). The inspection of ESR data shows the presence of ferric iron (III) as the only detectable oxidation state, with characteristic g factor of 2.435 and 2.615. The ferric iron signals at the above g values may be attributed to cubic Fe^{3+} , where the trivalent iron in $\alpha\text{-Fe}_2\text{O}_3$ may be coordinated by a distorted oxygen octahedron. The impregnation of Li^+ gave a hyperfine structure, which is hardly visible, presumably because of dipole-dipole interactions. Regarding the XRD patterns, for all investigated iron-containing samples, no evidence was found for the presence of ferrous iron (II) species or Fe^0 , agreeing with the recorded data for ESR technique.

Thermal analysis (TGA): TGA curves of the uncalcined TFIV and TFIV L10 samples show that the weight of the samples decreased in the N_2 gas stream in the temperature range of ~ 37.18 to 610°C . The total weight loss was 4.2 wt. % for TFIV and 16.8 wt.% for TFIV L20. Most of the weight loss may correspond to the removal of H_2O and NO_x . The curves comprise three distinguishable regions, indicating the weight loss upon temperature ramping. The first region represents the weight loss within the temperature interval $310\text{-}176^\circ\text{C}$, corresponding to the driven off physisorbed, bounded and constitutional water. The second weight loss at $449\text{-}363^\circ\text{C}$ may be referred to the thermal degradation of the impregnant, while the third stage terminated at 610°C may be attributed to the formation of $\gamma\text{-Fe}_2\text{O}_3$. The constant weight loss upon elevating the temperature beyond 610°C may be ascribed by the interconversion between the various phases of iron oxide (16, 20).

TGA curve of TFIV L10 sample behaved as TFIV sample with slight shift toward a high temperature for the first and second regions. Li^+ is well documented by its high affinity for water and therefore the removal of physisorbed, bounded and constitutional water may be delayed.

Surface acidity: The recommended adsorption of *n*-butylamine ($\text{pK}_a=10.73$) in non-aqueous media meets insurmountable agreements with a recent reported literature (14), where the irreversible adsorption of *n*-butylamine shows selectivity and superiority over other probe bases in estimating the number of acidic sites.

The chemical interaction of the n-butylamine-surface can be satisfactorily investigated by applying the langmuir adsorption equation:

$$C_e / Y = \frac{1}{bY_m} + \frac{C_e}{Y_m}$$

where C_e is the equilibrium concentration of n-butylamine, b is a constant, Y is the amount of n-butylamine adsorbed per gram of solid and Y_m is the monolayer coverage. The value of Y_m must be assumed as a measure of the acidic sites corresponding to specific pKa of n-butylamine.

The plot of C_e/Y vs. C_e gives a straight line with slope of $1/Y_m$ and the intercept of $1/bY_m$. The values of Y_m enable to calculate the acidity (number of acid sites/g), Table 2, column (6). The data given in Table 2 shows that the increase of iron content was accompanied with an increase in acidity, whereas the incorporation of Fe_2O_3 - TiO_2 system with Li^+ leads to an opposite behavior. The acidity of the investigated Fe_2O_3 - TiO_2 system may be caused by the substitution of Fe^{3+} into the structure of the host TiO_2 . The combination of oxides possessing different structures will be associated with a charge imbalance and creation of new acidic centers (1,2). The decrease of surface acidity upon impregnating with Li_2O may be due to the basic nature of this impregnant, leading to a partial neutralization of a fraction of surface acidity (21).

Catalytic activity measurements: The heterogeneous catalytic conversion of isopropanol can proceed via the dehydration and/or the dehydrogenation route(s), depending on the chemical nature of the catalyst. It has been reported that the formation of dehydration product (DHD) due to acidic sites, whereas the formation of dehydrogenation product (DHG) may arise from catalysis involving both an acid and a basic sites (22). In the present investigation, both propylene (P) as a dehydration product and acetone (A) as a dehydrogenation product were identified.

The data listed in Table 2 include the effect of reaction temperatures, iron oxide content, lithium oxide content and surface acidity on the catalytic activities of various solids. To determine which of the above mentioned products are really competitors, we used the term selectivity towards either DHD or DHG products,

where

$$\%S_P = \% \text{ propene} / (\% \text{ propene} + \% \text{ acetone}) \times 100$$

$$\%S_A = 100 - \%S_{DHD}$$

Table 2. % DHD and % DHG of 2-propanol and acid amounts of investigated samples

Temp. (C°)	360		340		320		300		Acid Amounts ×10 ⁻²¹
	%P	%A	%P	%A	%P	%A	%P	%A	
Catalyst									
TFI	24.7	2.40	17.3	0.00	9.80	0.00	6.60	0.00	2.80
TFII	27.5	7.00	21.8	1.60	11.6	0.50	7.70	0.00	2.90
TFIII	29.6	10.5	22.2	2.00	12.4	0.80	8.40	0.00	3.22
TFIV	31.2	13.1	23.8	3.20	13.0	1.80	9.50	0.00	3.37
TFV	37.7	18.8	30.1	9.60	20.3	4.20	12.2	0.00	3.44
TFIVL1	24.6	6.50	18.2	2.50	10.5	1.60			1.90
TFIVL3	19.1	7.00	14.3	2.40	7.40	1.50	Not traced		1.30
TFIVL6	15.5	6.20	10.4	2.50	6.30	1.80			1.00
TFIVL10	12.1	6.80	6.60	2.50	4.50	1.50			0.80

In a view for the catalytic conversion of 2-propanol depicted in Table 2, the following remarks are observed:

- (1) The dehydration and dehydrogenation activities as well as the total conversion increase with the increase of iron oxide content. This may be related to the increase of the active sites responsible for accelerating the DHD and DHG reactions.
- (2) The variation of % conversion and % selectivity with the reaction temperatures indicates the highest sensitivity of the products formed on the catalyst surface to the reaction temperatures.
- (3) The selectivity toward the dehydration decreased as the iron content increased. In contrast, the increase of iron content led to an increase of dehydrogenation selectivity. The increase of iron oxide content may reduce the ratio of Lewis to Bronsted acid sites and enhancing therefore the selectivity towards the dehydrogenation pathway, suggesting therefore the formation of acetone via β -elimination mechanism (4, 23).
- (4) Li-impregnated $\text{Fe}_2\text{O}_3\text{-TiO}_2$ sample gave a lower dehydration and dehydrogenation activities of 2-propanol conversion than that of Li-free samples. On the other hand, the successive increase of Li^+ was accompanied with steeping of the dehydrogenation activity and a decrease of dehydration. Percentage of conversion of 2-propanol vs. Li^+ content is shown. The depression of dehydration activity may be taken as an evidence for the removal of some surface acidity upon impregnating with alkali metal ions (21).

(5) The plot of % DHD vs. acidity expressed as acid amount gives a fairly good straight line. The back extrapolation of this line intersect the acid amount axis at a point, regarding the least number of acid sites required to initiate the dehydration reaction. The decrease of initial amount of acid sites required to start the DHD reaction with increasing reaction temperatures may be a guide for the importance in orienting the least number of acid sites to initiate the catalytic reaction (4).

For all investigated samples, the dehydrogenation of 2-propanol at constant temperature and different flow rate verified Bassett-Habgood's equation, depicting for the first order kinetics.

$$\ln 1/(1-X) = RTkKW/Q$$

Where X=fraction conversion, R=gas constant (atm. ml.k⁻¹.mole⁻¹), T = reaction temperature (K), k=adsorption constant of isopropanol on the catalyst (mol atm⁻¹ g⁻¹), K = rate constant of the surface process (s⁻¹), W = weight of catalyst (g) and Q = flow rate of carrier gas (ml s⁻¹). A representative plot of ln 1/(1-X) vs. 1/Q for TFIV sample gives a straight line passing through the origin, revealing that the reaction follows a first order kinetics.

Moreover, the result obtained for the dehydration reaction perfectly fit the Kiperman's equation :

$$X = k (1/V)^n$$

Where X is the fraction converted, k is the rate constant, V is the space velocity of reactant, and n is the overall order of reaction.

The plots of log X vs. log 1/V gives straight line, the slope of which is equal to the rate constant. From these foundations, it can be assumed that, under the experiment conditions, the reaction rate (r) can be equated by the rate equation:

$$r = \text{constant} [\text{propylene}]^n [\text{acetone}]$$

Where n is a fraction order.

According to Bassett and Habgood's kinetic relationship, one can obtain the pseudokinetic constant values (kK) at a constant temperature by plotting ln 1/(1-X) versus W, while the apparent activation energy (E_{a(Ap)}) can be obtained within the temperature range of 593-633 k from the plot of ln[ln(1/(1-X))] vs. 1/T. Table 3 shows the calculated catalytic parameters, namely kK and (E_{a(Ap)}):

Table 3. Catalytic parameters of 2-propanol decomposition

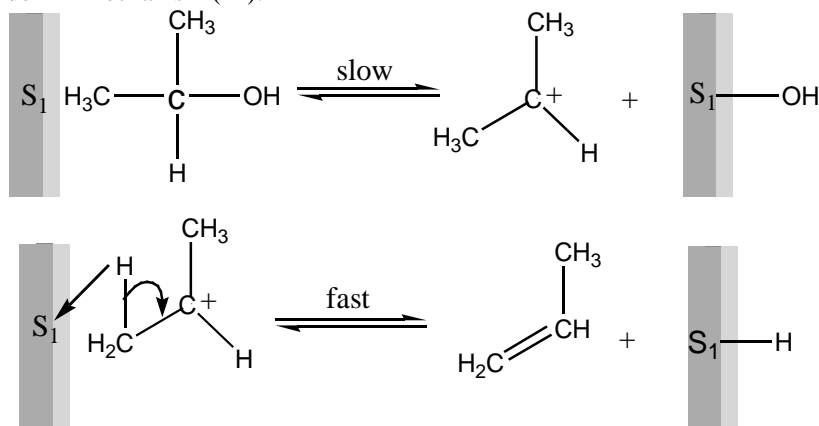
Parameters	Samples				
	TFI	TFII	TFIII	TFIV	TFV
$(E_{a(Ap)})$	65.75	111.48	108.42	84.05	66.13
kK-360°C	0.057	0.162	0.232	0.304	0.454
kK-320°C	0.022	0.033	0.049	0.071	0.166

The calculated values of apparent activation energy, using Arrhenius relationship, were found to be of 65.75-111.48 Kcal./mol. The values of kK increase gradually with the increases of iron oxide content, indicating on increase of the reaction rate in this trend. Moreover, the decrease of reaction temperature decreased the value of kK.

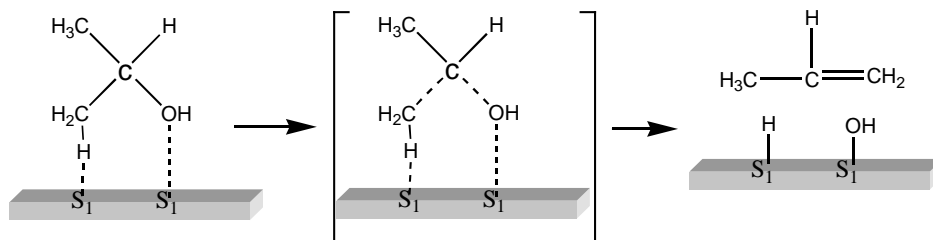
Reaction mechanism

The heterogeneous catalytic conversion of isopropanol can proceed, following three different mechanisms, depending on the acid/base nature of the catalyst surface. These mechanisms can be shortly noted as follow:

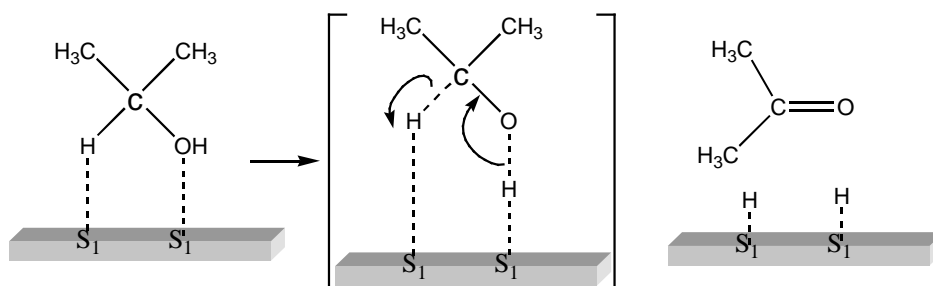
1. A unimolecular elimination mechanisms (E1), including the ionization of alcohol forming carbocation (rate determining step) and elimination of a β -proton to form alkenes. Such subsequent mechanism is confined to a highly acidic surface. For E1 type mechanism, the rate of the reaction should be a first order E1 mechanism (24):



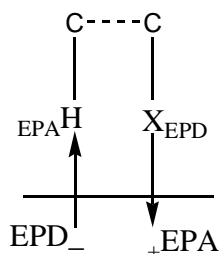
2. A bimolecular elimination mechanism (E2) involving the synchronous removal of both an OH group and a proton (24). For a constant concentration of isopropanol, the rate of the reaction may be expressed by the relationship: Rate = k [active sites], i.e. a first-order elimination process. Since the acidic and basic properties of the investigated solids were approximately identical, the E2 mechanism should be expected for the formation of alkenes.



3. For the solid catalyst having a large number of basic centers, an EICB mechanism can be assumed. This mechanism includes a displacement of a proton, followed by the removal of the leaving group (24). The mechanism of acetone production could be proposed as β -elimination mechanism (4, 23):



On the basis of coordination chemistry, the dehydration of alcohols may be considered to take place via the interaction of alcohols with two sites of acid-base nature, that can be schematically represented as follow:



One site is electron-pair acceptor (EPA) "Lewis acid" which involves an OH^- abstraction, while the other site is electron-pair donor (EPD) "Lewis base" which abstract H^+ , forming therefore alkene (23).

Conclusions

1. The textural parameters of T, TF and TFL, the impregnation of TF samples with Li^+ was associated with pronounced changes of the textural parameters, particularly at higher impregnant levels.
2. The XRD investigations of Fe^{3+} - impregnated titania samples indicated the presence of TiO_2 , Fe_2O_3 , and TiFe_2O_5 phases, while the impregnation of TF samples with Li^+ led to the formation of $\text{Li}_2\text{Fe}_2\text{O}_4$ spinel.
3. The increase of Fe^{3+} content was accompanied with an increase of surface acidity. In contrast, the basic nature of Li^+ reduces therefore of 32.1-71.4 % of the initial acidity.
4. The dehydration and dehydrogenation activities increases with the increase of iron oxide content, whereas the impregnation of TF with Li^+ led only to reduce of the dehydration activity.
5. The dehydration activity was found to be a fraction order kinetics, while the dehydrogenation activity followed a first order kinetics.
6. No significant correlation was found between the textural parameters and the dehydration/dehydrogenation activities.

References

- [1] Tanabe, K. In: *Catalysis by Acids and Bases*. Imelik B., Naccache, C., Coudurier, G., Ben Taarit, Y. and Vedrine, J.C. (Eds.), Amsterdam: Elsevier, 1985.
- [2] Tanabe, K. In: *New Solid Acids and Bases*, Vol. 51, Tanabe, K., Misono, M., Ono, Y. and Hattori, H. (Eds.), Kyo/Amsterdam: Kodansha/Elsevier, 1989.
- [3] Youssef, A.M. and El-Sharkawy, E. A. "Oxidation of Carbon Monoxide over Supported Metal Oxide Catalysts." *Ads. Sci. Technol.*, 12 (1995), 335.
- [4] El-Sharkawy, E. A. "Textural, Structural and Catalytic Properties of $\text{ZnCr}_2\text{O}_4/\text{Al}_2\text{O}_3$ Catalysts." *Ads. Sci. Technol.*, 16, No. 3(1998), 193.
- [5] Shengcheng, Luo and John, L. "Falconer, Acetone and Acetaldehyde Oligomerization on TiO_2 Surfaces." *J. Catal.*, 18, No. 5 (1999), 393.
- [6] Boccuzzi, F., Guglielminotti, E., Martra, G. and Cerrato, G. "Nitric Oxide Reduction by CO on Cu / TiO_2 Catalysts." *J. Catal.* 6 (1994), 449.
- [7] Angeles, Larrubia, M., Gianguido, R. and Guido, B. "An FT-IR Study of the Adsorption and Oxidation of N-containing Compounds Over $\text{Fe}_2\text{O}_3\text{-TiO}_2$ SCR Catalysts." *J. Appl. Catal. B: Environmental*, 1 (2001), 101.
- [8] Boccuzzi, F., Chiorino, A., Gargano, M. and Ravasio. "Crotonaldehyde Hydrogenation on Pt / TiO_2 and Ni / TiO_2 SMSI Catalyst." *J. Catal.*, 5 (1997), 40.
- [9] Bonamali, P., Tomohiro, H., Kouichi, G. and Gyoichi, N. "Photocatalytic Degradation of α -Cresol Sensitized by Iron-Titania Binary Photocatalysts." *J. Mol. Catal. A: Chemical*, 169, No. 1 (2001), 147.
- [10] Martin, C. "Physicochemical Properties of WO_3/TiO_2 System for 4- Nitrophenol Degradation in Non aqueous Media." *Catal. Letter*, 49, No. 3 (1997), 235.
- [11] Dhananjay, S.B., Vishwas, G.P. and Beenackers, Anthony, A.C.M.B. "Photocatalytic Degradations for Environmental Applications: A Review." *J. Chem. Technol. & Biotechnol.*, 77, No. 1 (2002), 102.
- [12] Youssef, A.M., Samra, S.E., Abou El-Nadar, H.M. and El-Sharkawy, E.A. "Surface and Catalytic Properties of Aluminas in Relation to the pH of Precipitation." *Bull. Soc. Chim.Fr.*, 128 (1991), 604.
- [13] El-Sharkawy, E.A., Mostafa, M.R. and Youssef, A.M. "Surfaces and Catalytic Properties of $\text{SnO}_2 - \text{Cr}_2\text{O}_3$ Catalysts." *Ads. Sci. and Technol.*, 15, No. 3 (1997), 237.
- [14] El-Hakam, S.A. and El-Sarkawy, E.A. "Structural Characterization and Catalytic Properties of Aluminium Borates-alumina Catalysts." *Materials Letters*, 36 (1998), 167.
- [15] Gregg, S. J. and King, K.S.W. *Surface Characteristics*. London: Academic Press Inc., 1982, p. 45.

- [16] El-Sharkawy, E.A., El-Hakam, S.A. and Samra, S.E. "Effect of Thermal Treatment on the Various Properties of Iron (III) -Aluminum (III) Coprecipitated Hydroxide Systems." *Materials Letter*, 42 (2000), 331.
- [17] El-Hakam, S.A., El-Khouly, A.A. and Khder, A. S., *Ads. Sci. & Technol.*, 17 (1999), 417.
- [18] *X-Ray Powder Diffraction Files of Inorganic Compounds*. Edited by JCPOS International Center for Diffraction Data, 1978.
- [19] Mabbs, F. E. and Collision, D. "Electron Paramagnetic Resonance of d Transition Metal Compounds." Amsterdam: Elsevier, 1992.
- [20] Mani, B. and Sitakara Rao, V. "Structural and Phase Changes in Iron (III)- Aluminum (III) Mixed Hydroxide-Oxide System; A: Thermoanalytical Study." *Therm.Chem. Acta*, 53 (1982), 175.
- [21] Vinek, Hannelore. "Dehydration and Dehydrogenation Reactions over Al_2O_3 , SiO_2 and Alkali Impregnated Al_2O_3 and SiO_2 ." *Z. Phys. Chem.*, (Munich) (1980), 121.
- [22] Mars, P. *The Mechanism of Heterogeneous Catalysis*. de Boer, J.H. (Ed.). Amsterdam: Elsevier, 1959, p. 49.
- [23] El-Sharkawy, E.A. *Surface and Catalytic Properties of Chromia-silica Catalysts*. Ph.D Thesis, Mansoura University, Egypt, 1994.
- [24] Finar, I.L. *The Fundamental Principles of Organic Chemistry*.Vo. 1. Singapore: Longmans, 1973, 162.

نزع الماء-الهيدروجين من كحول ٢- بروبانول باستخدام حفّازات أكسيد الحديد-التيّتانيا: تأثير التشريب بأيون الليثيوم

السيد عبدالعظيم الشراوي السقا و شار سعد الشهري

قسم الكيمياء، كلية العلوم، جامعة الملك فيصل، ص. ب ١٧٥٩،

الهفوف ٣١٩٨٢، المملكة العربية السعودية

(قدم للنشر في ١٨/٢/١٤٢٣هـ؛ وقبل للنشر في ٢٢/١٢/١٤٢٣هـ)

ملخص البحث. تم تحضير حفّازات أكسيد الحديد المحمّل على التيتانيا بنسب ١-٣٥% من الحديد وذلك بطريقة تشريب التيتانيا سابقة التحضير بنترات الحديد عند درجة حرارة ٣٣٣ كيلفن وأتبع ذلك بالتجفيف والتحميص عند درجة حرارة ٨٧٣ كيلفن. كذلك أكسيد الحديد/التيتانيا المشربة بالليثيوم ١-١٠% تم تحضيرها بنفس الطريقة. درست الخواص النسيجية عن طريق امتزاز النيتروجين عند درجة حرارة ٧٧ كيلفن. تم فحص الخواص التركيبية للعينات المحمّصة باستخدام تقنيات حيود الأشعة السينية وجهاز التحليل التقاضي الحراري وجهاز التحليل الوزني الحراري وجهاز الطنين الإلكتروني المغزلي. درست حمضية أسطح الحفّازات بامتزاز البيوتيل أمين العادي في الهكسان الحلقي كوسط غير مائي. استخدمت تقنية النبض الميكروحفزي لدراسة الخواص الحفزية وكذلك حركية التفاعلات: تفاعلات نزع الماء - نزع الهيدروجين من كحول ٢ - بروبانول. لقد أوضحت النتائج ما يلي:

تقل المعاملات التركيبية المقاسة كمساحة السطح وحجم المسام الكلي بزيادة نسبة الحديد أو الليثيوم. دلّت دراسة حيود الأشعة السينية للحفّازات المحضّرة وجود أطوار مختلفة من التيتانيا وأكسيد الحديد وكذلك مزيج من مركب يحتوى التيتانيا وأكسيد الحديد، وكذلك الليثيوم وأكسيد الحديد. أوضحت دراسة الرنين الإلكتروني المغزلي وجود أيون الحديد الثلاثي في كل العينات المحتوية على الحديد. تزداد حمضية السطح بزيادة نسبة الحديد وتقل بزيادة نسبة الليثيوم. تتأثر الخواص الحفزية بكل من النسبة المئوية للحديد و/ أو الليثيوم في أكاسيدها وكذلك حمضية السطح للحفّازات المحضّرة.

